Structural Elucidation of Soluble Polyelectrolyte–Micelle Complexes: Intra- vs Interpolymer Association

Jiulin Xia, Huiwen Zhang,[†] Daniel R. Rigsbee, Paul L. Dubin,* and Tehseen Shaikh

Department of Chemistry, Indiana University–Purdue University at Indianapolis, Indianapolis, Indiana 46205-2820

ABSTRACT: Soluble complexes formed between the strong polycation poly(dimethyldiallylammonium chloride) and mixed micelles of sodium dodecyl sulfate/Triton X-100, in 0.40 M NaCl and at low polymer concentration and excess surfactant concentration, were investigated by a variety of techniques. The results of turbidimetry, static light scattering, dynamic light scattering, dialysis equilibrium, viscometry, and electrophoretic light scattering are discussed in terms of possible structures for the complex in the limit of low polymer concentrations (C_P), and its tendency to associate upon an increase in C_P. The findings from these various studies are consistent with the formation of an intrapolymer complex at low C_P. In this species, the binding of numerous mixed micelles leads to charge reversal and to the formation of a highly extended chain, wherein the dominant influence on polymer dimensions is intermicellar repulsion.

Introduction

Polyelectrolytes form complexes with oppositely charged mixed micelles.[1-11] Whether or not association takes place appears to depend only on the micelle surface charge density σ, the polymer linear charge density ξ, and the Debye–Hückel ion-atmosphere thickness κ^{-1}.[7,11] The corresponding experimental variables are the fraction of surfactant head groups in the micelle which are charged (Y), the structural polymer charge density $1/b$ (where b is the distance between charges on the polymer chain), and the ionic strength I. Y is controlled experimentally by adjusting the bulk stoichiometry of the surfactant mixture. For a given polyelectrolyte in some particular ionic strength medium, i.e. at constant b and I, a critical surfactant mole fraction Y_c—corresponding to a critical micelle surface charge density—is observed; for $Y < Y_c$ no association takes place[1,3,6] regardless of the concentration of polymer, C_P, or total surfactant, C_S. To the first order, Y_c is also independent of polymer molecular weight (MW).[5] Beyond this phase transition point, the system may form soluble polyion–micelle complexes, liquid coacervate, or amorphous precipitate.[4] The nature of the complex phase, unlike the conditions for incipient complexation, does depend on C_p, C_s, and MW,[4,5] as well as on the other three variables mentioned.

The structure of soluble polyelectrolyte–micelle complexes is of interest for several reasons. Systems in which polyelectrolytes are adsorbed on the surface of oppositely charged colloids are usually biphasic, but a number of polyelectrolyte–micelle complexes constitute reversible, equilibrium aggregates whose properties may be examined by a wide range of techniques. The effects on the configuration of the adsorbed polymer of inter alia colloid surface charge density, colloid curvature, ionic strength, and polymer charge density may therefore be studied in a variety of ways not possible in truly biphasic systems. From another point of view, polyelectrolyte–micelle complexes represent a degree of self-organization that is remarkable in purely abiotic systems: surfactant molecules, organized in micelles, are bound within the domains of a polyelectrolyte chain, which then may or may not form a higher-order aggregate.[9] In some cases, it appears that a particular association state is much preferred, and

the way in which a combination of hydrophobic and electrostatic forces leads to the stabilization of one particular structure has obvious relevance to the understanding of natural supramolecular assemblies. A final question arises regarding the influence of the relative sizes of the colloid and the polymer. Polymer–micelle complexes have been described as a "necklace of beads",[12] a model that obviously breaks down when the micelle size approaches that of the polymer. It is of interest to consider whether there is a structural discontinuity in the region where the ratio of micelle dimensions to polymer dimensions exceeds unity, and whether the overall structure depends on the absolute or the relative sizes of the two macroionic species.

The range of conditions in which soluble complexes are stable is particularly wide in the system composed of the strong polycation poly(dimethyldiallylammonium chloride) (PDMDAAC), the anionic surfactant sodium dodecyl sulfate (SDS), and the nonionic surfactant Triton X-100 (TX100), in aqueous NaCl solution. Under such conditions, we have previously characterized soluble complexes by viscometry,[1] turbidimetry,[1,3,5,7] quasielastic light scattering (QELS),[2,3,10] and static light scattering,[8] mainly at $I = 0.40$ M. While these investigations have shed some light on the properties of these species, a well-defined picture of the complex structure has not emerged. Previous QELS measurements on the complex in the polymer concentration range $0.2 < C_p < 1$ g/L suggest that the mean apparent Stokes radius ($\bar{R}_S{}^{app}$) of the complex is on the order of 40–70 nm, while the polymer alone exhibits $\bar{R}_S{}^{app} = 17 \pm 2$ nm.[10,11] From somewhat preliminary static light scattering[8] we found R_g for the micelle-free polymer of 40 ± 5 nm (in 0.4 M NaCl); for the complex formed with micelles at $Y = 0.35$, we found $R_g \geq 40$ nm, with considerable sensitivity to the concentration range over which the data were gathered. Under these conditions, the weight-average molecular weight of the complex was more than 20 times larger than that of the polymer alone (2×10^5). Thus, the very large ratio of mass to dimensions seemed to suggest that the complex is very compact.

Despite the foregoing findings, the data available do *not effectively discriminate* among hypothetical structures such as those shown in Figure 1. The structures shown in Figure 1 may be described as intrapolymer (1A and 1B) or interpolymer (1C) complexes. In 1A, neutralization of
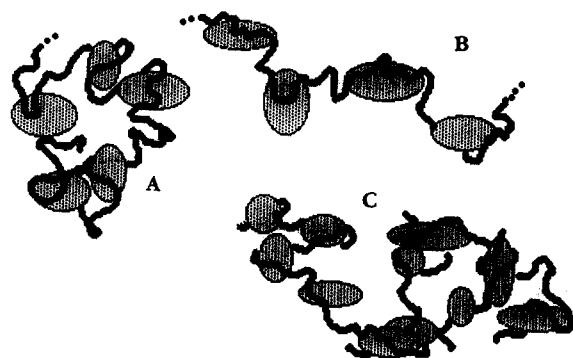
Figure 1. Models for soluble complexes of PDMDAAC with mixed micelles of SDS/TX100: (A) intrapolymer complex in which the polymer dimensions are reduced by micelle binding; (B) extended intrapolymer complex; (C) multipolymer (interpolymer) complex.

the polyion charges by association with micelles reduces the intersegmental repulsion and there is some collapse of the polymer chain. In 1B, the repulsive forces among micelles is considered to be a dominating effect and the polymer assumes a more extended configuration than in the absence of surfactant.

A central unanswered question is whether intrapolymer complexes, resembling those proposed by Cabane for complexes of poly(ethylene oxide) and SDS micelles,[12] exist under any conditions. Such an intrapolymer complex might then undergo further association to form higher-order complexes. On the other hand, complexes might always be multipolymer and rather polydisperse. Considerations of this type are relevant to the general question of how it is that stable intermacromolecular complexes of finite size are formed. The ambiguity in interpreting the previous results arose in part from the variability of the polymer concentration ranges hitherto employed for the different techniques. In the current work, we report further on turbidimetry, QELS, and static light scattering measurements collected over a wider range of conditions, particularly at very low polymer concentrations. The influence of micelle surface charge density on complex structure has also been explored. In addition, electrophoretic light scattering measurements were carried out to investigate the influence of the number of bound micelles and their average charge state on the charge state of the complex. We have also used dialysis equilibrium to gain some insight into the polyelectrolyte–micelle binding phenomenon and more detailed viscometry than in previous measurements. Taken together, these results lead to a clearer picture of the nature of the aggregated state.

Experimental Section

Materials. Poly(dimethyldiallylammonium chloride) (PDMDAAC) (trade name Merquat 100) was from Calgon Corp. (Pittsburgh, PA) and was dialyzed (12 000–14 000 nominal MW cutoff) and freeze-dried before use. Sodium dodecyl sulfate (SDS) was Puriss grade from Fluka (Happague, NY). Triton X-100 (TX100) was from Sigma (St. Louis, MO). All water was deionized and distilled.

Turbidimetry. Turbidity measurements were made at 420 nm with a Brinkmann PC800 probe colorimeter, equipped with a 2.0-cm path length fiber optics probe. "Type 1" titrations were carried out at 24 °C by adding 60 mM SDS in 0.40 M NaCl, with a micrometer buret, to a solution of 40 mM TX100 and PDMDAAC of the desired concentration, also in 0.40 M NaCl, and recording $100 - \% T$ (nearly linear with the turbidity for $\% T > 90$). All such values were corrected by subtraction of the turbidity of a polymer-free blank.

Quasielastic Light Scattering. Samples for QELS were prepared by mixing stock solutions of the individual components

and filtering with Gelman (Ann Arbor MI) 0.2-μm syringe filters directly into the appropriate cell. The light source for QELS was a 20-mW HeNe laser from Jodon (Ann Arbor, MI). Measurements were made at a 90° scattering angle with a Brookhaven (Holtsville, NY) system equipped with a 72-channel digital autocorrelator (BI-2030 AT). The quality of the measurements was verified by determining that the measured experimental baseline of the time correlation function of concentration fluctuations, $g(q,t)$, was within 1% of the calculated one. The distribution of diffusivities and hence the size distribution function was obtained by inverse Laplace transformation using the program CONTIN.[13] Additional measurements were obtained with a system composed of a Malvern RR102 spectrometer and a Nicomp TC-100D autocorrelator (Santa Barbara, CA) interfaced to an Epson Equity II+ through Procomm version 2.3 communication software. Photon counts were acquired until the "fit error" and "residual"[14] were less than 2 and 5, respectively. In part to show that the apparent size distributions were reproducible and not dependent on deconvolution algorithms, measurements were also made with a Coulter (Hialeah, FL) Model N4MD. N4MD run times were 5 min, with parameters chosen automatically at each of the three scattering angles, 30, 60, and 90°. Descriptions of the principles and practice of QELS may be found in refs 15 and 16.

Static Light Scattering (SLS). One set of SLS measurements were made with an Otsuke Photoal DLS-700 instrument (Polymer Labs, Amherst MA). The preparation of solutions was as follows. SDS/TX100 mixed micelle solutions were prepared in 0.40 M NaCl at the desired total surfactant concentration (C_S) and mole fraction of SDS (Y) and filtered through 0.20-μm Gelman filters (Ann Arbor, MI). PDMDAAC in 0.40 M NaCl was added to attain the desired polymer concentration C_P. Samples were filtered repeatedly through 0.20-μm Anotec disposable filters. Temperatures varied from 25.9 to 26.7 °C from one run to another but were constant within ±0.1 °C during any particular run. The Otsuke instrument measures the time and angle dependence of the scattered intensity of each solution, which greatly facilitates the identification and rejection of dusty samples. Measurements were made from 40 to 150° scattering angles, and dedicated software was used to adjust the scaling factor k and to plot the results.

Essentially identical techniques were used to prepare samples for SLS measurements with the Brookhaven instrument described above. The static scattering intensities, I_S, were measured as the photon count rates at scattering angles from 30 to 150° with a 200-μm pinhole aperture for the EMI photomultiplier tube. The average of 10 such measurements was reported as I_S. These values were used to construct the Zimm plot.

Construction of Zimm plots for complexes formed in situ poses several serious problems.[17] First, while the concentrations of the components—micelles and polymer—are known, the mass concentration of the complex is not. A related problem is the selection of the reference solvent for determination of background scattering. A third difficulty is the possibility that the complex structure is concentration-dependent, obscuring the interpretation of Zimm plots. We adopted the following procedure to address these problems. With regard to the last matter, the concentration of surfactant used was 14 g/L, in large excess compared to polymer concentration ($0.002 < C_p < 0.01$ g/L). We expected that these conditions would saturate polymers with micelles and tend to ensure that the composition of complexes would be invariant with C_p. Since some of the surfactant is polymer-bound, the solution is depleted in free surfactant by the amount $C_s' = \beta C_p$, where β is the mass of surfactant bound per unit mass of polymer. β is not directly determined, but is a useful parameter because it relates the molecular weight of the complex to the weight concentration of the complex. The latter quantity, required for preparation of the Zimm plot, is $C_x = C_p(1 + \beta) \simeq \beta C_p$, where free polymer is assumed to be of negligible concentration. If complexes were intrapolymer, then $\beta = (M_x - M_p)/M_p \simeq M_x/M_p$, where M_x and M_p are the average molecular masses of complex and polymer, respectively. Thus, in the case of intrapolymer complexes, C_x and M_x are not independent variables, since $C_x/C_p = M_x/M_p = \beta$. If each complex were to contain N polymer chains, then $\beta = (M_x - NM_p)/NM_p \simeq M_x/NM_p$ (the molar mass of the complex is in fact always found to be quite large

compared to any reasonable value of NM$_P$).

The choice of the reference solvent was dictated by the need to maintain a constant concentration of all species save the complex. Ideally, the reference solvent should be the external dialysis solution of the scattering sample, but this would require use of a membrane permeable to micelles, but not to polymer or complex, and many weeks for equilibration (see below). Under the conditions of this study (0.40 M NaCl) the micelle size is not far enough below that of the polymer to ensure that dialysis equilibrium of the former species can be attained without transport of the latter. Instead, to maintain concentration of unbound surfactant of 14.0 g L^{-1}, we enhanced the total surfactant concentration of each solution by $C_s' = \beta C_p$, which was first estimated by guessing a value for β. Since the value for β determines C_x, we may then, after collection of data, plot in the usual way KC_x/R_θ vs $\sin^2(\theta/2) + kC_x$. The resultant Zimm plot yields an approximation of M_x which may be or may not be consistent with the original choice of β. If it is not, we obtain a second estimate of β and C_x. After two such iterations (including adjustments in added surfactant βC_p) the results converged to a stable value of M_x. The precision for β was estimated as about ±20%; β values outside this range yielded distorted Zimm plots as well as M_x values that were not self-consistent with the Zimm plots.

Electrophoretic Light Scattering (ELS). Electrophoretic light scattering was carried out at 25 °C, at four scattering angles (8.6, 17.1, 25.6, and 34.2°) using a DELSA 440 apparatus (Coulter Instrument Co., Hialeah, FL). The electric field was applied at a constant current of 10 mA. An electrophoretic cell with a square cross section, connecting the hemispherical cavities in each electrode, was used. The total sample volume was about 1.0 mL. The measured electrophoretic mobility was the average value obtained at the stationary layer for the four scattering angles. A discussion of the principles of ELS may be found in ref 18.

Dialysis Equilibrium. Dialysis equilibrium studies were performed with cells of our own design.[19] Homemade two-component dialysis cells with an effective capacity of 5.6 mL on each side of a 0.02-μm Anopore membrane disk (Alltech Assoc, Deerfield, IL) were used to separate PDMDAAC-bound and free SDS/TX100 micelles. To compartment one was added with a Finnpipette (Cole Scientific, Woodland Hills, CA) 5.6 mL of the aqueous polymer solution (1.0 g/L). To compartment two were added SDS/TX100 solutions of varying concentrations. After a magnetic stir bar was placed in each compartment, the cells were sealed by parafilm O-rings between the membrane and the cells. The sealed cells were secured by rubber bands and placed on a magnetic stirrer at 22 °C for 50 days to reach equilibrium, at which time the concentration of the SDS/TX100 in compartment two no longer changed with time. Then, 2.0-mL samples were taken from compartment two for UV–vis spectrophotometry (HP-8450) to determine the equilibrium free SDS/TX100 concentration in the system, since the concentrations of free surfactant in both compartments are the same at equilibrium.

Viscometry. Efflux times were measured with reproducibilities of ±0.05 s or better in a Ubbelohde type glass viscometer operated as part of a Shott AVSN automatic viscometer (Schott Glaswerke, Mainz), in a 30.0 ± 0.1 °C bath. Efflux times were measured in 0.40 M NaCl for (a) PDMDAAC at varying concentrations, (b) SDS-TX100 at varying concentrations, at Y = 0.40, and (c) PDMDAAC at varying concentrations, in SDS-TX100 at 29.2 g/L, for Y = 0.24 and 0.27. Severe difficulties were encountered as foam interfered with detection of the meniscus and could only be overcome with considerable care and patience.

Results and Discussion

Turbidimetry. Figure 2 shows type 1 titrations at I = 0.40 in 40 mM TX100, at varying polymer concentrations in the range 0.01 g/L < C_p < 1.0 g/L. The point of initial increase in turbidity is designated as Y_c and occurs at Y = 0.23 at this ionic strength regardless of polymer or total surfactant concentration.[20] Such curves exhibit maxima between Y_c and Y_p when C_p > ca. 0.5 g/L; the magnitude of these "humps" most likely reflects the formation of
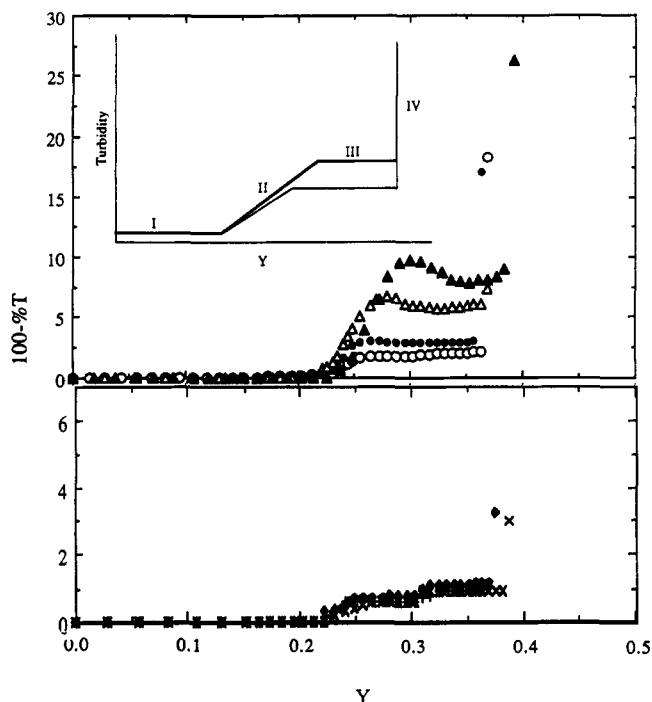

Figure 2. "Type 1" turbidimetric titration of PDMDAAC in 0.40 M NaCl, at polymer concentrations of (A, top) (from top to bottom) 1.0, 0.60, 0.30, and 0.10 g/L and (B, bottom) (from top to bottom) 0.06, 0.03, and 0.01 g/L. Insert: schematic illustrating three regimes of polyion–micelle interaction.
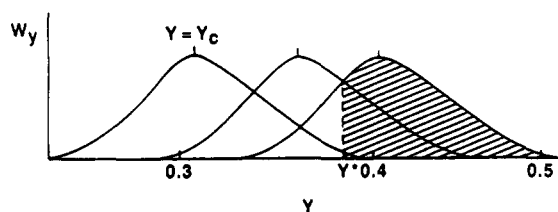

Figure 3. Schematic depiction of hypothetical mixed micelle compositional distributions at different values for the bulk (macroscopic) mole fraction of SDS. Y^* represents the microscopic critical micelle composition, while the abcissa corresponds to microscopic (micellar) composition. The shaded areas represent the fraction of micelles that participate in binding to the polymer. Thus, for a bulk SDS mole fraction of Y = 0.31, "active" micelles begin to appear; hence Y_c = 0.31. Adapted from ref 1.

higher-order complexes.[9] When such humps are absent, the type 1 curves exhibit three regimes, as shown by the schematic in the insert of Figure 2A. In region I, the surface charge density of the micelles, σ, is not sufficient to lead to complex formation. Region II is best explained on the basis of micelle compositional polydispersity, recognizing that the stoichiometric mole fraction Y is an average value, from which the compositions of individual micelles will vary. This polydispersity is depicted in Figure 3, a hypothetical plot of the weight fraction as a function of microscopic mole fraction. In this figure, $Y \cong 0.38$ is arbitrarily chosen as the microscopic micellar critical composition: individual micelles with the mole fraction of SDS equal to or exceeding this quantity bind to the polycation. The number concentration of such "active" micelles with sufficient charge for binding first exceeds zero when the measured (bulk) $Y = Y_c$; the fraction of micelles that are active increases with Y and then achieves a limiting value, corresponding respectively to regions II and III in the insert of Figure 2. Under the conditions of excess surfactant employed here, the plateau corresponds to the regime in which additional active micelles are added but cannot be accommodated in the already saturated
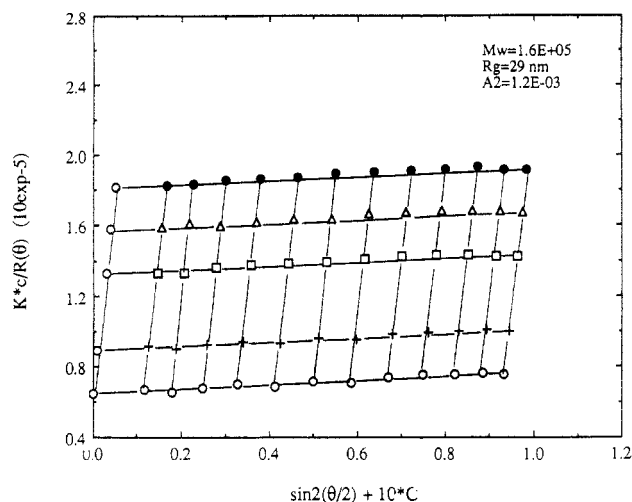
Figure 4. Zimm plot for PDMDAAC in 0.40 M NaCl.

Table I. Light Scattering Results for PDMDAAC and for SDS/TX100 Mixed Micelles, in 0.40 M NaCl

	$\bar{M}_w$	R_g, nm	R_S^{app}, nm	ρ	A_2, mol mL/g^2
PDMDAAC	$1.5^5 \times 10^5$	$28.^7$	15	1.9	$1.1^7 \times 10^{-3}$
SDS/TX100 Y = 0.28			9		
SDS/TX100 Y = 0.32	$1.9^4 \times 10^5$	$21.^6$	$9.^5$	2.3	$-2.2^5 \times 10^{-4}$
SDS/TX100 Y = 0.36	$1.9^0 \times 10^5$	$22.^2$	9	2.5	$-3.5^5 \times 10^{-4}$

complexes, so the addition of SDS does not lead to an increase in the number or size of scatterers. With progressive addition of SDS, an abrupt increase in turbidity signals bulk phase separation. This observation may be explained on the basis of more efficient and more intimate ion-pairing between the polymer and the micelle at high σ, accompanied by release of small ions and concomitant desolvation and insolubilization of the complex.

Static and Dynamic Light Scattering. While the results of Figure 2 only permit qualitative hypotheses about complex structure, they serve to guide further light scattering measurements. We suggest that the maxima in the curves at $C_p > 0.5$ g/L correspond to higher-order aggregation;[9] contrariwise, it appears likely that such aggregation is less important in the range $C_p < 0.5$ g/L and that the structure of the complex could be constant with respect to polymer concentration under these conditions. Static light scattering (SLS) and dynamic light scattering of mixtures of PDMDAAC and SDS/TX100 were therefore conducted in 0.40 M NaCl, at low polymer concentrations $0.002 < C_p < 0.01$. The total surfactant concentration was maintained near 14 g/L, corresponding to a TX100 concentration of about 25 mM.

Zimm plots for PDMDAAC and SDS/TX100 ($Y = 0.32$), both in 0.40 M NaCl, are presented in Figures 4 and 5,

respectively. The increment of refractive index of PDMDAAC was taken as 0.186, as determined by Burkhardt.[21] The refractive index of SDS/TX100 was measured as 0.137, using a differential refractometry calibrated with sucrose standards, as described elsewhere.[8] Additional measurements were made for SDS/TX100 at $Y = 0.28$ and 0.35. Light scattering results for PDMDAAC and the mixed micelles are summarized in Table I. The ratio of the radius of gyration to the Stokes radius, ρ, is also included, because there is considerable theoretical basis for interpretation of this quantity in terms of polymer chain compactness.[22]

It is of interest to compare the static light scattering results with earlier findings from QELS.[3,5] The 2-fold difference between R_g and R_S^{app} observed for PDMDAAC is expected for polyelectrolytes.[23] (This behavior is observed for the complex as well, as shown below.) With regard to the micelle, we note that the axial ratio of an ellipsoid with a hydrodynamic radius of 10 nm (as observed) and a minor radius of 5 nm (the value of R_S^{app} found for TX100) is about 2,[24] so these results are consistent with a moderately elongated micelle. Although the size of the mixed micelles at this ionic strength goes through a shallow maximum with Y,[25] micelle dimensions are nearly constant with respect to surfactant composition over the range $0.28 < Y < 0.35$ of interest here. These compositions were chosen because, as suggested by Figure 2, saturation of the complex occurs at $Y > 0.25$, $Y = 0.28$ is close to the turbidimetric maxima seen for $C_p > 0.5$ g/L, and minima occur in the range $0.32 < Y < 0.35$.

SLS and QELS of the complex formed between the mixed micelle and PDMDAAC were carried out under these conditions by the procedures described above. Attempts to measure dn/dc of the complex with a differential refractometer failed because of turbidity
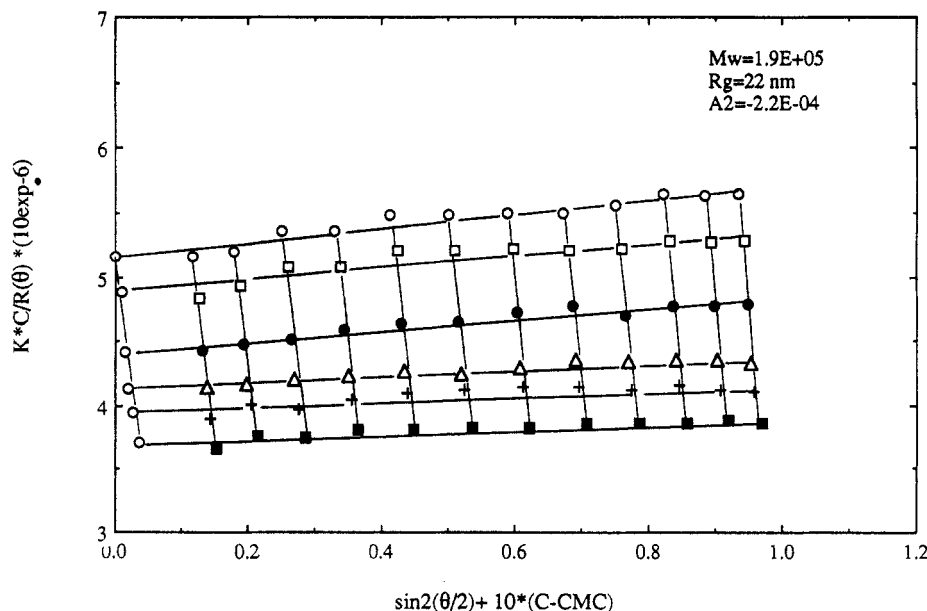

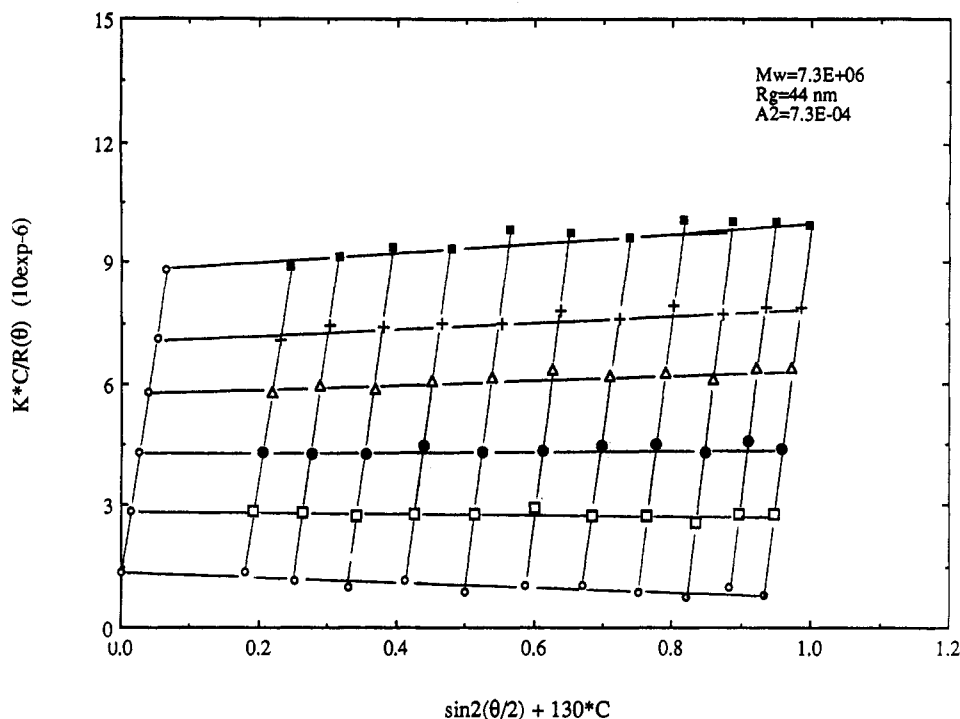**Figure 5.** Zimm plot for SDS/TX100 at $Y = 0.32$, in 0.40 M NaCl.

Figure 6. Zimm plot for the complex formed between PDMDAAC and mixed micelles of SDS/TX100 at $Y = 0.28$, in 0.40 M NaCl.

Table II. Light Scattering Results for Complexes Formed between PDMDAAC and SDS/TX100 Micelles of Varying Composition in 0.40 M NaCl

Y	$10^6 M_w$	R_g, nm	R_S^{app}, nm[a]	ρ	$10^4 A_2$, (mol mL)/g^2
0.28	7.3[4]	44.[3]	20.[5]	2.2	7.[4]
0.32	10.[3]	51.[0]	25	2.0	9.[3]
0.36	15.[1]	52.[5]	25	2.1	5.[9]

[a] $C_p = 0.01$ g/L.

effects. Since the complex is composed of polymer and micelle, $(dn/dc)_x$ of the complex may be written as[26]

$$\left(\frac{dn}{dc}\right)_x = \frac{1}{1+\beta}\left(\frac{dn}{dc}\right)_p + \frac{\beta}{1+\beta}\left(\frac{dn}{dc}\right)_m \qquad (1)$$

where the subscripts x, p, and m represent complex, polymer and micelle, respectively. β represents the mass ratio of bound micelle to polymer. According to the observed large turbidity, $\beta \gg 1$ is expected. Therefore, we used the value of $(dn/dc)_m$ in eq 2 for $(dn/dc)_x$.[27] The resulting Zimm plot is shown for $Y = 0.28$ in Figure 6. Data of similar quality were obtained at $Y = 0.32$ and 0.36. Parallel QELS measurements were made at $C_p = 0.01$ g/L, under identical conditions of I and Y. In order to obtain the size of the complexes, the correlation functions were fitted according to a two-exponential decay, as given by

$$g(t) = a_1 \exp(-D_1 q^2 t) + a_2 \exp(-D_2 q^2 t) \qquad (2)$$

where q is the amplitude of the scattering vectors, D_1 and $D2$ are the diffusion coefficients for the free micelle and complex, respectively, and a_1 and a_2 are constants. From each value of D we obtain the Stokes radius R_S from the Einstein equation

$$R_s = kT/6\pi\eta D \qquad (3)$$

where k is the Boltzmann constant, T the absolute temperature, and η is the viscosity of the solvent. QELS results are summarized in Table II.

From the data in Tables I and II, we observe that the dimensions of the complex are on the order of 50–70% larger than the polymer's. On the other hand, the molecular masses are greater than those of either micelle

or polymer by factors of 35–100. This result suggests a high degree of compactness for the complex. On the other hand, the quantity $\rho = R_g/R_S$ increases from 1.9 for the polymer alone, to 2.1 ± 0.1 for the complex. From theory, ρ is 0.778 for hard spheres and is predicted to be 1.5 for flexible chains in a Θ-solvent and 1.78 for flexible chains in a good solvent. The value of ρ may be expected to be significantly larger for polyelectrolytes, as observed for PDMDAAC. For ellipsoids with appreciable axial ratios, such as the (polymer-free) mixed micelles, $\rho > 2$ is easily attained. The fact that β values for the complex are intermediate between those of the polymer and the micelle suggests that the complex is more extended than the free polymer.

It is of interest to note that the mass increases by 50% as Y increases from 0.32 to 0.36, while the dimensions are unchanged. This must be explained by an increase in the micelle binding constant, which increases the mean number of bound micelles. As recently pointed out by Stahlberg et al.[29] the binding of a macroion to an oppositely charged surface includes a repulsive osmotic term: the lack of charge symmetry between the two surfaces along with the requirement for electroneutrality means that some counterions must reside between the two surfaces, so there is an osmotic effect that keeps the surfaces apart. In the present case that leads to a rather loose binding between the high linear charge density polycation and the lower charge density mixed micelle. We suggest that charge symmetry is more nearly attained upon an increase in Y. This leads to stronger micelle binding, and therefore an increase in the number of bound micelles per polymer chain, and hence an increase in complex $\bar{M}_w$.

Electrophoretic Light Scattering. ELS results for mixed micelles and for complexes with PDMDAAC, in 0.40 M NaCl, are shown in Figure 7. As expected, the mobility of the complex is less negative than that of the mixed micelle and, in fact, is zero close to the point of the inception of binding, Y_c. The mobility of the micelle is seen to be a linear function of Y. Since the mobility is the ratio of the charge to the friction factor, we can write for
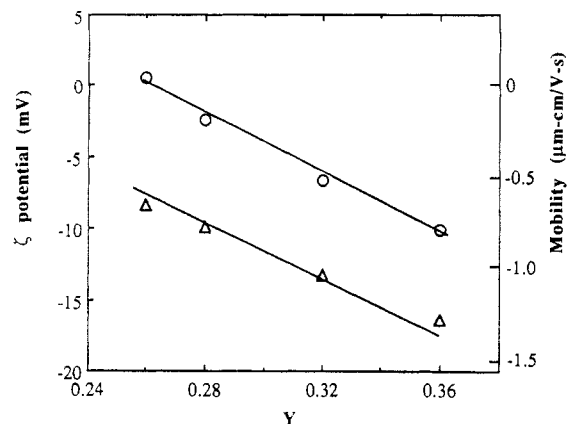
Figure 7. Electrophoretic mobility and ζ potential of SDS/TX100 micelles (lower curve) and the PDMDAAC-SDS/TX100 complex (upper curve), both in 0.40 M NaCl. Polymer concentration, 0.001 g/L; TX100, 3.0 mM.

the micelle mobility

$$U_m = \frac{q_m}{f_m} = -\frac{n_{av}eY}{f_m} \tag{4}$$

where n_{av} is the mean micellar aggregation number and e is the electronic charge and where the effect of counterion binding to the micelle is neglected. The linear dependence of U_m on Y indicates that there is little change in n_{av} or f_m with Y, consistent with the MW and R_S results in Table I. The Y dependence of the mobility of the complex is nearly linear and, interestingly, is displaced by almost a constant amount from the curve for the micelles. If we assume that the mobility of the complex is the sum of contributions from the bound micelles and the polymer and we assert that the contribution of N bound micelles to the friction factor is simply Nf_m, then we can write

$$U_x = \frac{q_p}{f_p + Nf_m} - \frac{Nn_{av}eY}{f_p + Nf_m} \tag{5}$$

where U_x is the mobility of the complex, q_p is the net charge of the polymer, f_p is the polymer contribution to the friction factor of the complex, and N is the number of micelles bound per polymer chain. The difference between the mobilities of the complex and the micelle is then

$$\Delta U = \frac{q_p f_m + n_{av}ef_p Y}{f_m(f_p + Nf_m)} \tag{6}$$

Since the charge on the polymer, q_p, is larger by about a factor of 10 than the charge on the micelle, $n_{av}eY$, and f_p is not very much larger than f_m, the first term in the numerator of eq 6 is large relative to the second, and ΔU does not show much dependence on Y. From the large MW of the complex, we know that N is large, therefore $Nf_m \gg f_p$. Then eq 5 reduces to

$$U_x \cong \frac{q_p}{f_p + Nf_m} - \frac{n_{av}eY}{f_m} \tag{7}$$

The weak curvature in the U_x vs Y plot can best be explained by an increase in N with Y. This is consistent with the fact that the MW of the complex doubles as Y increases from 0.28 to 0.36, as shown in Table II. Counterion binding to the micelle, neglected in the preceding analysis, may also be one reason for the curvature.

The complex is electrically neutral at $Y = 0.26$. From this result we may estimate N, as follows. The micelle aggregation number is about 350 with a corresponding

formal net charge of about 90. If the complex contains a single polymer chain with a net charge of about 1200, then the number of bound micelles required to compensate this charge is approximately 15. The mass of this hypothetical complex would be about 3 million. A rough extrapolation from the MW values of the complex obtained at $Y = 0.28$, 0.32, and 0.38 to $Y = 0.26$ is about 5 million. This calculation makes a number of assumptions, including the hypothesis that the bound micelle has the same structure as the free one; dye solubilization studies do suggest that there is no major restructuring of the micelle on complex formation. A second, and less likely, assumption is the absence of counterion binding to the micelle. Evidence from Figure 7 against this supposition is seen as follows. A linear extrapolation of the data for the micelle to lower Y gives the unlikely result of zero mobility at $Y = 0.15$; in fact, the plot must exhibit curvature at lower Y to keep this from happening. While such effects can be partly due to changes in micelle size and shape,[25] it also seems likely that the ratio of micelle charge to aggregation number is not a linear function of Y because of counterion binding. Other studies on mixed micelle systems (mainly at low ionic strength) suggest a decrease in the degree of cation "dissociation" α with ionic surfactant content.[30] Reduction of the net charge of bound micelles by a decrease in α increases the complex MW calculated via the charge neutrality argument made above, bringing that estimate even closer to the observed value.

With increasing Y, the electrophoretic mobility becomes progressively more negative, as would be expected. However, the magnitude of the change in U is greater than would be predicted from the increasingly negative micelle charge; i.e. the slope of the curve for the complex is larger than that for the micelle alone. As pointed out above, this can best be understood in terms of an increase in the number of micelles bound per polymer chain, corresponding to an increase in the micelle–polyion binding constant with increasing Y. This change is reflected in dialysis equilibrium results, as described below.

Dialysis Equilibrium. On the basis of the assumption that the concentration of unbound micelles on the polymer side of the dialysis cell is the same as the total concentration of micelles on the polymer-free side of the membrane, we can determine the concentration of bound and free micelles in the polymer compartment. The high ionic strength employed allows us to neglect the Donnan effect in the analysis of the dialysis data. Figure 8A presents the results obtained at a polymer concentration of 1 g/L, in 0.40 M NaCl, for $Y = 0.32$ and 0.38, as a plot of the mass of bound surfactant (as millimoles of TX100) per gram of polymer, Q, vs surfactant concentration C_S. Taken at face value, the results suggest a saturation at [TX100] > 25 mM (i.e. above $C_S = 17$ g/L total surfactant). In the case of $Y = 0.32$, the saturation value of $Q = 7$ is consistent with only 4–5 micelles bound per polymer chain, which calls into question either the MW obtained by static light scattering or the assumption that the complex involves a single polymer chain. This result also contradicts electrophoretic light scattering results, because complexes in which the number of bound micelles per polymer chain is less than 10 cannot have a net negative charge. There is reason to believe that saturation is not attained under the conditions of the dialysis equilibrium experiment when the weight ratio of total surfactant to polymer is $C_S/C_P = 30$ (the upper limit of conditions in Figure 8A). Furthermore, the large size of the micelles ($R_S^{app} = 9$ nm at $Y = 0.34$) reduces the rate of dialysis and thus the certainty that equilibrium has been attained. Figure 8B displays results obtained at a lower polymer concentration, 0.15 g/L, at $Y = 0.14$ and
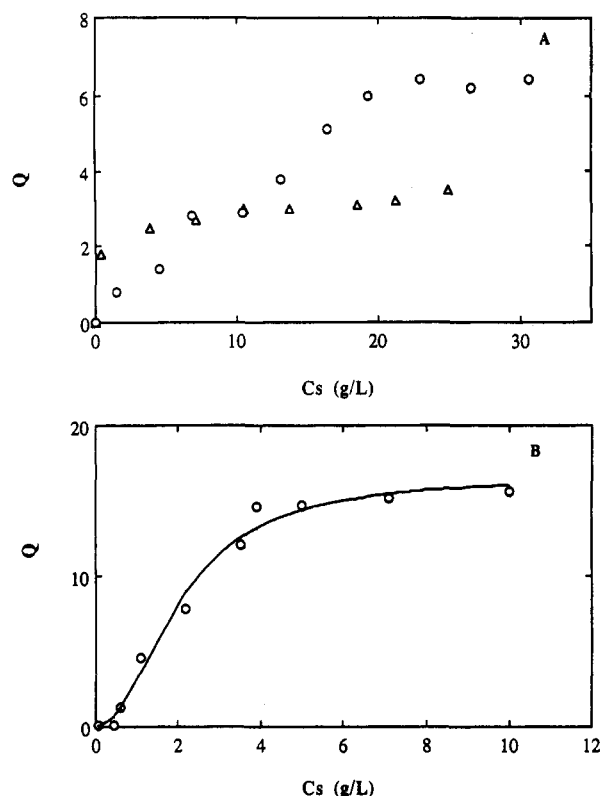
Figure 8. Dialysis equilibrium results, presented as Q, concentration of bound surfactant, reported as millimolar TX100 bound per gram of polymer, vs total surfactant concentration: (A) polymer concentration $C_P = 1$ g/L, $Y = 0.32$ (O) and 0.38 (△), in 0.40 M NaCl; (B) $C_P = 0.15$ g/L, $Y = 0.14$, in 0.10 M NaCl. The solid line in (B) is the best fit to Hill's equation.

$I = 0.10$ M (at this lower value of Y, the micelles are smaller, which therefore accelerates the approach to dialysis equilibrium). The results (obtained after 50 days of dialysis) are well fit by Hill's equation[31]

$$Q = \frac{k_1 C_s^z}{1 + k_2 C_s^z} \qquad (8)$$

shown by the solid line in Figure 8B for $z = 2.4$, $k_1 = 3.7$, and $k_2 = 0.2$. The value of $z > 1$ indicates that the binding is cooperative, and the saturation value of $Q = 15$, obtained at $C_S/C_P \simeq 50$ g/g, is consistent with approximately 20 micelles bound per polymer chain.

The light scattering, electrophoresis, and viscosity experiments are carried out at—or extrapolated to—C_S/C_P in excess of 500. It is impossible to carry out the dialysis experiment under the same conditions for technical reasons: the change in UV absorption in the polymer-free cell is two small to measure with precision. We must then recognize that the dialysis experiments correspond to stoichiometries different than those in the light scattering/hydrodynamic studies and the structures of the complexes formed under these two different sets of conditions may differ. Although the dialysis technique merits further exploration, at this time it may not contribute to the structural characterization of the complex formed at infinite dilution of polymer, in excess micelle.

Viscometry. Plots of reduced specific viscosity vs concentration are shown in Figure 9 for (a) mixed micelle, (b) PDMDAAC, and (c) complex. In the last case, complex is formed by isoionic addition of polymer to a solution of SDS-TX100. If the concentration used is that of polymer alone, an intrinsic viscosity of 160 cm³/g for the polymer in mixed micelle "solvent" is obtained, i.e. 3 times greater than $[\eta]$ in 0.40 M NaCl. However, the addition of polymer
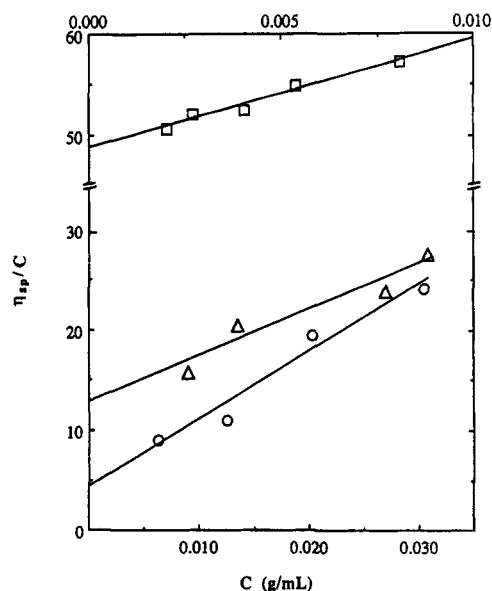

Figure 9. Viscosity plots for (□) PDMDAAC (axis above), (O) SDS/TX100 ($Y = 0.30$),. and (△) the complex of PDMDAAC in SDS/TX100 at $Y = 0.30$, 40 mM TX100 (see text for explanation). All are in 0.40 M NaCl.

may be viewed as an increase in the concentration of the complex, along with a diminution of the surfacant concentration of the solvent medium. Assuming $\beta = 36$ (as determined from light scattering), we can calculate the effective mass concentration of the complex, i.e. $C_P\beta$, which is the concentration used for the complex in constructing the viscosity plot of Figure 9. We must also correct for the reduction in solvent viscosity that comes from the removal of surfactant upon complex formation. This correction was performed by using the viscosity of the effective micellar solvent as the solvent viscosity. The effective micellar solvent is a pure micelle solution with a micelle concentration of $C_m - C_p\beta$, where C_m and C_p are the concentrations of the micelle and polymer, respectively, in the complex solution. The value of $C_m - C_p\beta$ is the free micelle concentration in the complex solution. With this correction, we obtain the viscosity plots shown in Figure 9, along with $[\eta] = 13$ cm³/g for the complex. This intrinsic viscosity is remarkably small, which suggests a high degree of compactness. However, it is important to point out that "compactness" deduced from low $[\eta]$ means that the effect on solution viscosity *per unit mass* of solute is small, and this may arise either from reduced chain dimensions or, as is more likely in the present case, from large mass per contour length. We may use the measured viscosity in conjunction with the molecular weight as obtained from light scattering to calculate the viscosity radius as[32]

$$R_\eta = (3M[\eta]/10\pi N_A)^{1/3} \qquad (9)$$

This quantity is sometimes referred to as "the equivalent hydrodynamic radius" but we prefer the term "viscosity radius" in order to avoid confusion with the dimension obtained from diffusivity, the Stokes radius. Both R_S and R_η are "equivalent" dimensions, since they are based on theories for spheres, but are nevertheless of demonstrated utility. Using for the molecular weight the value of 7×10^6 measured at $Y = 0.28$ in Table II, we obtain $R_\eta = 24$ nm, very nearly in agreement with the Stokes radius of 21 nm measured by dynamic light scattering for the complex at $Y = 0.28$. Thus the low value of $[\eta]$ is compensated for by the large value of M; this result is consistent with a chain with a moderately large persistence length, but with a large ratio of mass to hydrodynamic volume.

Speculations on the Structure of the Soluble Complex at Low Polymer Concentration.

There is clear evidence for the formation of higher aggregates at large solute concentration, which may be envisioned as the precursors of coacervation.[9] In this work we focus on the complexes formed at low C_P; with the exception of the dialysis experiments, all results refer to $C_P < 0.5$ g/L. These complexes are extremely massive, with $\bar{M}_w$ ranging from 7 to 15 million as Y increases from 0.28 to 0.36. For an intrapolymer complex, these values would correspond to an increase in the number of bound micelles per polymer chain from 35 to 70 upon an increase in Y. Under the same conditions both the Stokes radius and the radius of gyration increase about 20%, i.e. from about 50% larger than the value for the free polymer to 60–80% larger. At $Y = 0.24$ and 0.27, the intrinsic viscosity measurements correspond to viscosity radii in good agreement with the Stokes radii. The electrophoretic mobilities show that the extent of micelle binding at $Y = 0.25$ is sufficient to completely neutralize the polymer charge, and a further increase in Y causes a rapid increase in the magnitude of the (negative) ζ-potential of the complex.

The extraordinarily high $\bar{M}_w$ values seen at large Y might seem to suggest a multipolymer complex; however it would be difficult to understand how such a complex could exhibit the stability with respect to aggregation in the limit of very low polymer concentration that would be necessary to yield regular Zimm plots. Furthermore, the positive second virial coefficient of the complex is not consistent with a highly self-aggregating system. These results and the good agreement between the hydrodynamic radii obtained in the limit of zero C_P from viscometry, and at $C_P = 0.01$ g/L from QELS, suggest that the complex structure is invariant in this C_P range, which is more consistent with an intrapolymer structure. In order to explain the magnitude of R_g and $R_S{}^{app}$, we refer to the extended intrapolymer structure of Figure 1B. Although the hydrodynamic dimensions of the free polymer are not a great deal larger than those of the free micelle, it is important to keep in mind that the contour length of the polymer is ca. 50–100 times larger than either of these.

In the limit of excess surfactant, saturation of the polymer with micelles can be attained, especially at high Y. The intense binding of the micelles to the polymer produces, via steric and electrostatic intermicellar repulsive effects, a strong chain expansion and near-doubling in R_g. To conceptualize the structure of the complex in an intuitively reasonable manner, we may imagine that micelles tend to be oriented with their major axes parallel to the average direction of the local bound polymer segments, in order to minimize their surface curvature in the vicinity of the bound polymer chain. The chain itself is highly extended on a local scale but, because of the high ionic strength, exhibits flexibility at distances that are large compared to the micelle dimensions. The same intermicellar repulsions that produce chain expansion also lead to interparticle repulsion, and the second virial coefficient for the complex is positive, and just ca. 50% smaller than A_2 for PDMDAAC. In contrast to PDMDAAC, the mass:contour length ratio is very large.

References and Notes

(1) Dubin, P. L.; Oteri, R. *J. Colloid Interface Sci.* **1983**, *95*, 453.

(2) Dubin, P. L.; Davis, D. D. *Macromolecules* **1984**, *17*, 1294.

(3) Dubin, P. L.; Rigsbee, D. R.; McQuigg, D. W. *J. Colloid Interface Sci.* **1985**, *105*, 509.

(4) Dubin, P. L.; Davis, D. D. *Colloids Surf.* **1985**, *13*, 113.

(5) Dubin, P. L.; Rigsbee, D. R.; Gan, L. M.; Fallon, M. A. *Macromolecules* **1988**, *21*, 2555.

(6) Dubin, P. L.; Thé, S. S.; McQuigg, D. W.; Chew, C. H.; Gan, L. M. *Langmuir* **1989**, *5*, 89.

(7) Dubin, P. L.; Curran, M. E.; Hua, J. *Langmuir* **1990**, *6*, 707.

(8) Dubin, P. L.; Thé, S. S.; Gan, L. M.; Chew, C. H. *Macromolecules* **1990**, *23*, 2500.

(9) Dubin, P. L.; Vea, M. E. Y.; Fallon, M. A.; Thé, S. S.; Rigsbee, D. R.; Gan, L. M. *Langmuir* **1990**, *6*, 1422.

(10) Rigsbee, D. W.; Dubin, P. L. *J. Soc. Photo-Opt. Instrum. Eng.* **1991**, *1430*, 1430.

(11) McQuigg, D. W.; Kaplan, J. I.; Dubin, P. L. *J. Phys. Chem.* **1992**, *96*, 1973.

(12) Cabane, B.; Duplessix, *J. Phys.* **1982**, *43*, 1529.

(13) Provencher, S. W. *Comput. Phys. Commun.* **1982**, *27*, 229.

(14) In the Nicomp software, "fit error" is obtained from the square of the errors between the fitted and measured autocorrelation functions, normalized with respect to particle size, while "residual" is the coefficient obtained for the decay constant of an infinitely large particle, commonly attributed to "dust events".

(15) Pecora, R.; Gerne, B. *J. Dynamic Light Scattering*; Wiley: New York, 1986.

(16) Stock, R. S.; Fay, W. H. *J. Polym. Sci., Polym. Phys. Ed.* **1985**, *23*, 1393.

(17) See, for example: Dautzenberg, H.; Rother, G. *J. J. Polym. Sci., Appl. Polym. Symp.* **1991**, *48*, 351.

(18) Ware, B. R.; Haas, D. D. *Fast Methods in Physical Biochemistry and Cell Biology*; Shaafi, R. I., Fernandez, S. M., Eds.; Elsevier: Amsterdam, 1983.

(19) Rigsbee, D. R. Thesis. Purdue University, in preparation.

(20) Fallon, M. A. Thesis. Purdue University, 1986.

(21) Burkhardt, C. W.; McCarthy, K. J.; Parazak, D. P. *J. Polym. Sci., Polym. Lett. Ed.* **1987**, *25*, 209.

(22) (a) Burchard, W.; Schmidt, M.; Stockmayer, W. H. *Macromolecules* **1980**, *13*, 1265. (b) Schmidt, M.; Stockmayer, W. H. *Macromolecules* **1984**, *17*, 509.

(23) Wang, L.; Yu, H. *Macromolecules* **1988**, *21*, 3498.

(24) Richards, E. G. *An Introduction to the Physical Properties of Large Molecules in Solution*; Cambridge University Press: Cambridge, U.K., 1980; p 164. Thé, S. S. Thesis. Purdue University, 1989.

(25) Dubin, P. L.; Principi, J. M.; Smith, B. A.; Fallon, M. A. *J. Colloid Interface Sci.* **1989**, *127*, 558.

(26) Patkowski, A.; Bujalowski, W.; Chu, B. *Biopolymers* **1982**, *21*, 1503.

(27) The effect of this approximation on $\bar{M}_w$ for the complex (M_x) is difficult to assess directly; however, in separate work in 0.10 M, under which conditions the mixed micelle is small enough to allow dialysis equilibrium studies,[28] the number of micelles bound per polymer chain so determined was in good agreement with M_x in that solvent. This is circumstantial evidence for the validity of this approximation.

(28) Rigsbee, D. R.; Xia, J.; Dubin, P. L. Unpublished results.

(29) Stahlberg, J.; Jönsson, B.; Horvath, C. *Anal. Chem.* **1991**, *63*, 1867.

(30) Ogino, K.; Abe, M. In *Mixed Surfactant Systems*; Holland, P. M., Rubingh, D. N., Eds.; ACS Symposium Series 501; American Chemical Society: Washington, DC, 1992; Chapter 8.

(31) Hill, A. V. *J. Physiol.* **1910**, *40*, 190.

(32) Flory, P. J. *Principles of Polymer Chemistry*; Cornell University Press: Ithaca, NY, 1953; p 606.